Measurement of electrons from semileptonic heavy-flavor hadron decays in pp collisions at √s=2.76 TeV

(STAR Collaboration) Abelev, B.; ...; Antičić, Tome; ...; Gotovac, Sven; ...; Mudnić, Eugen; ...; Planinić, Mirko; ...; ...

Source / Izvornik: **Physical Review D - Particles, Fields, Gravitation and Cosmology, 2015, 91**

Journal article, Published version
Rad u časopisu, Objavljena verzija rada (izdavačev PDF)

https://doi.org/10.1103/PhysRevD.91.012001

Permanent link / Trajna poveznica: https://urn.nsk.hr/urn:nbn:hr:217:145216

PHYSICAL REVIEW D **91,** 012001 (2015)

Measurement of electrons from semileptonic heavy-flavor hadron decays in *pp* collisions at $\sqrt{s} = 2.76$ TeV

B. Abelev *et al.*[*]
(ALICE Collaboration)

(Received 3 June 2014; published 7 January 2015)

The p_T-differential production cross section of electrons from semileptonic decays of heavy-flavor hadrons has been measured at midrapidity in proton-proton collisions at $\sqrt{s} = 2.76$ TeV in the transverse momentum range $0.5 < p_T < 12$ GeV/c with the ALICE detector at the LHC. The analysis was performed using minimum bias events and events triggered by the electromagnetic calorimeter. Predictions from perturbative QCD calculations agree with the data within the theoretical and experimental uncertainties.

DOI: 10.1103/PhysRevD.91.012001 PACS numbers: 13.85.Qk, 13.20.Fc, 13.20.He, 13.75.Cs

I. INTRODUCTION

The measurement of the production of heavy-flavor hadrons, i.e. hadrons carrying charm or beauty quarks, in proton-proton (pp) collisions provides a test of quantum chromodynamics (QCD), the theory of the strong interaction. In hadronic collisions, heavy quarks are almost exclusively produced through initial hard partonic scattering processes because of their large masses [1]. Consequently, the heavy-flavor hadron production cross sections are calculable in the framework of perturbative QCD (pQCD) down to very low transverse momenta (p_T).

Furthermore, heavy-flavor production cross sections measured in pp collisions provide a reference for corresponding measurements in high-energy nucleus-nucleus collisions, in which the formation of a strongly interacting partonic medium has been observed [2–9]. Heavy quarks are produced on short time scales, presumably before this medium is formed. Consequently, they probe the medium properties while they propagate through it [10–13]. In particular, the color charge and mass dependence of the partonic energy loss can be studied by comparing the suppression of heavy-flavor hadrons and hadrons carrying light quarks only [14,15].

One available method to investigate heavy-flavor production is the measurement of the contribution of semileptonic decays of heavy-flavor hadrons to the inclusive electron spectra. This contribution is substantial because of branching ratios of the order of 10% into the semielectronic decay channel [16] and the large heavy-quark production cross sections at LHC energies [17,18]. In pp collisions at $\sqrt{s} = 7$ TeV, the signal of electrons from heavy-flavor hadron decays is of similar magnitude as the background [19] at an electron transverse momentum of ≈ 2 GeV/c, and the ratio of signal to background increases with p_T.

The production of heavy-flavor hadrons was studied at the LHC in pp collisions at $\sqrt{s} = 7$ TeV in various channels by ALICE [17–21], ATLAS [22–24], CMS [25–31], and LHCb [32–35]. Perturbative QCD calculations [36–40] describe the measurements within the uncertainties.

For a center-of-mass energy of 2.76 TeV, which is the reference energy for Pb-Pb collisions in 2010 and 2011 at the LHC, ALICE already reported on the production of muons from heavy-flavor hadron decays in pp collisions at forward rapidity [13], and reconstructed open charm mesons at midrapidity [41]. Again, pQCD calculations describe the experimental data reasonably well. This paper presents a measurement of electrons, $(e^+ + e^-)/2$, from semileptonic decays of charm and beauty hadrons in the transverse momentum range $0.5 < p_T < 12$ GeV/c at midrapidity in pp collisions at $\sqrt{s} = 2.76$ TeV using the ALICE detector. The analysis technique employed here is similar to the one described in detail in [19], where the measurement in pp collisions at $\sqrt{s} = 7$ TeV is presented, and it consists of the following steps: selection of electron candidates, subtraction of the remaining hadron contamination, correction for efficiency and normalization, and subtraction of the electron background originating from non-heavy-flavor sources.

II. EXPERIMENTAL SETUP AND DATA SET

The ALICE experiment at the LHC is described in detail in [42], thus we only briefly introduce the detectors relevant for this analysis.

The detector closest to the interaction point is the Inner Tracking System (ITS). It consists of six cylindrical layers, grouped into three subsystems. The Silicon Pixel Detector (SPD) equips the two innermost layers, placed at radii of 3.9 and 7.6 cm from the beam axis. The spatial resolution of the detector is 12 μm in the transverse plane ($r\varphi$) and

[*] Full author list given at the end of the article.

100 μm along the beam direction. The SPD is followed by two layers of the Silicon Drift Detector (SDD) and two layers of the Silicon Strip Detector (SSD) at radii between 15 and 43 cm.

A large cylindrical Time Projection Chamber (TPC), which is the main tracking detector, surrounds the ITS at a radial distance between 85 and 247 cm. The chamber's volume is filled with a mixture of Ne (85.7%), CO_2 (9.5%), and N_2 (4.8%) as drift gas. In the radial direction, the readout is divided into 159 pad rows. The TPC covers a pseudorapidity range of $|\eta| < 0.9$ for tracks having space points in the outermost pad rows. The specific energy deposit $\mathrm{d}E/\mathrm{d}x$ is used to identify particles. The $\mathrm{d}E/\mathrm{d}x$ resolution of the TPC ($\sigma_{\mathrm{TPC}-\mathrm{d}E/\mathrm{d}x}$) is approximately 5.5% for minimum ionizing particles passing through the full detector [43].

The tracking detectors are housed inside a solenoidal magnet providing a homogeneous magnetic field of 0.5 T. The ITS and the TPC provide a transverse momentum measurement for charged particles with a resolution of $\approx$1% at 1 GeV/c and $\approx$3% at 10 GeV/c [44].

The Time-of-Flight Detector (TOF) is located at a distance of 3.7 m from the beam axis covering the full azimuth and $|\eta| < 0.9$. The resolution of the particle arrival time is better than 100 ps. The collision time (t_0) is measured with the T0 detector, an array of Cherenkov counters positioned at $+370$ and -70 cm, respectively, along the beam axis. In case no information from the T0 detector is available, the collision time is estimated using the arrival time of the particles in the TOF detector. If also this second method does not provide a t_0 measurement, the bunch crossing time from the LHC is used [41]. Particles are identified using the difference between the measured time of flight and the expected time of flight for a given particle species, normalized to the overall time-of-flight resolution $\sigma_{\mathrm{TOF\text{-}PID}} \approx 150$ ps [41], including both the resolution of the particle arrival time measurement and of the t_0.

The Electromagnetic Calorimeter (EMCal) is a sampling calorimeter based on Shashlik technology spanning the pseudorapidity range $|\eta| < 0.7$ and covering 107° in azimuth [45]. The azimuthal coverage was limited to 100° for the data presented here. The EMCal supermodules comprise individual towers each spanning $\Delta\varphi \times \Delta\eta = 0.0143 \times 0.0143$ (6×6 cm). Each 2×2 group of neighboring EMCal towers forms a trigger elementary patch. The energy resolution was measured to be $1.7 \bigoplus 11.1/\sqrt{E(\mathrm{GeV})} \bigoplus 5.1/E(\mathrm{GeV})\%$ [46], where $\bigoplus$ indicates a sum in quadrature.

The V0 detector, used for online triggering and offline event selection, consists of two arrays of 32 scintillator tiles on each side of the interaction point. The detectors cover $2.8 < \eta < 5.1$ and $-3.7 < \eta < -1.7$, respectively.

The data used in this analysis were recorded in the spring of 2011. Two different data samples are available: a minimum bias sample and a sample triggered by the EMCal. In both samples, the SDD information was read out only for a fraction of the recorded events. The minimum bias trigger required at least one hit in either of the V0 detectors or the SPD. Background from beam-gas interactions was eliminated using the timing information from the V0 detector and the correlation between the number of hits and the reconstructed track segments in the SPD [47]. Events were required to have a reconstructed primary vertex [44] within ± 10 cm from the center of the detector along the beam direction. This covers 86% of all interactions. Pileup events were identified as events having multiple vertices reconstructed in the SPD and they were rejected in this analysis. The probability of pileup events was less than 2.5% in this data sample. The amount of remaining pileup events after rejection was negligible in this analysis [19]. Before further event selection the minimum bias sample consisted of 65.8 M events, corresponding to an integrated luminosity $L_{\mathrm{int}} = 1.1\ \mathrm{nb}^{-1}$. The use of the TOF information for particle identification required a stricter run selection which limited the integrated luminosity to $0.8\ \mathrm{nb}^{-1}$ (43.8 M events). In addition to the minimum bias sample, events selected by the EMCal trigger were analyzed. It required the coincidence of the minimum bias trigger condition described above and an energy sum in 2×2 EMCal trigger patches (4×4 towers) exceeding nominally 3 GeV. After event selection, the data sample recorded with the EMCal trigger corresponded to an integrated luminosity of $L_{\mathrm{int}} = 12.9\ \mathrm{nb}^{-1}$.

III. ANALYSIS

The minimum bias data sample was analyzed employing electron identification based on the information from the TPC [48]. At low transverse momentum ($p_{\mathrm{T}} < 2$ GeV/c) additional information from the TOF detector was required to improve the rejection of hadronic background. Electron identification in the analysis of the EMCal triggered data sample was based on the combined information from the TPC and the EMCal. The three analyses employing TPC, TPC-TOF, and TPC-EMCal electron identification, were conducted in different kinematical regions. In transverse momentum, the TPC analysis was restricted to the range $2 < p_{\mathrm{T}} < 7$ GeV/c, the TPC-TOF analysis was performed in the range $0.5 < p_{\mathrm{T}} < 5$ GeV/c, and the TPC-EMCal analysis was done in the range $2 < p_{\mathrm{T}} < 12$ GeV/c. In the latter case, the analysis used the minimum bias data sample for electron transverse momenta below 5 GeV/c and an EMCal triggered data sample for electron p_{T} above 4 GeV/c. In p_{T} regions where the cross sections have been determined from more than one analysis the results were found to be consistent within uncertainties. Results from individual analyses were adopted for three different p_{T} ranges. At low p_{T} (up to 2 GeV/c), the TPC-TOF analysis provides the purest electron candidate sample. In the range $2 < p_{\mathrm{T}} < 4.5$ GeV/c, the result from the TPC analysis has smaller systematic uncertainties than both

results from the TPC-TOF and the TPC-EMCal analyses. At high p_T (above 4.5 GeV/c), the TPC and TPC-TOF analyses are statistics limited and the TPC-EMCal analysis of the EMCal triggered data sample provides the smallest uncertainty.

Reconstructed tracks were selected for the analysis using the criteria listed in Table I, which are similar to those used in the analysis described in [19]. In particular, the cut on the minimum number of ITS clusters was reduced to three (instead of the value of four used in [19]) because the SDD points, which were not available for a sizable fraction of the events, were excluded from the track reconstruction used for this analysis, thus limiting the maximum number of hits in the ITS to four. In order to reduce wrong associations between candidate tracks and hits in the first layer of the SPD, hits in both layers of the SPD were required in the TPC-TOF analysis. In the TPC-EMCal analysis, this requirement has been relaxed to at least one hit in any of the two SPD layers in order to increase the statistics, thus resulting in a larger background. A cut on the minimum distance to the primary vertex was not imposed because electrons from charm hadron decays are indistinguishable from electrons originating from the primary vertex.

Three methods were used to identify electrons: in both the TPC and the TPC-TOF analyses, electrons were identified via their specific energy deposition (dE/dx) in the TPC. Tracks were required to have a dE/dx between one standard deviation below and 3 standard deviations above the expected dE/dx of electrons, consistent with an electron identification efficiency of ≈85%. In the TPC analysis for $p_T \geq 2$ GeV/c, a more stringent cut was applied in order to cope with the increasing hadron contamination towards higher momenta. Therefore, electron candidate tracks were required to have a dE/dx between 0.5 standard deviations below and three standard deviations above the mean dE/dx for electrons, corresponding to a selection efficiency of ≈70%. For $p_T < 2$ GeV/c, in the TPC-TOF analysis, the TOF detector was used in addition to the TPC. Here tracks were required to have a time of flight consistent with the expected time of flight for electrons within 3 standard deviations $\sigma_{\text{TOF-PID}}$, thus rejecting protons and kaons at momenta where they cannot be distinguished from electrons via dE/dx alone.

For $p_T \geq 4.5$ GeV/c, the TPC-EMCal analysis was employed. In the TPC, a dE/dx between 1.4 standard deviations below and 3 standard deviations above the mean dE/dx for electrons was required, corresponding to an electron identification efficiency of ≈90%. Tracks were extrapolated from the TPC to the EMCal surface and geometrically associated with EMCal clusters within 0.02 both in η and in φ. The ratio of the energy of the matched cluster in the EMCal to the momentum measured with the TPC and ITS (E/p) was required to be within 0.8 and 1.4 for electron candidates, corresponding to an identification efficiency of ≈60% averaged over p_T.

The hadronic background was estimated using a parametrization of the TPC dE/dx in various momentum slices [19] or, alternatively, the E/p distribution of identified hadrons, and it was subtracted from the electron candidate sample. For the TPC-TOF/TPC analysis the hadron contamination was negligible for $p_T \leq 2$ GeV/c and less than 1.5% for $p_T \leq 4.5$ GeV/c. In the TPC-EMCal analysis, the hadron contamination was negligible for $p_T \leq 6$ GeV/c, remained below 10% for $p_T \leq 8$ GeV/c, and it increased to ≈40% at $p_T = 12$ GeV/c.

The p_T-differential invariant yield of inclusive electrons per minimum bias event has been obtained by dividing the raw yield of electrons, $(e^+ + e^-)/2$, measured in p_T bins of widths Δp_T, by the number of minimum bias events, by $2\pi p_T^{\text{center}}$ where p_T^{center} is the value of p_T at the center of each bin, by Δp_T, by the width Δy of the covered rapidity interval, and by the product of the geometric acceptance ϵ^{geo}, the reconstruction efficiency ϵ^{reco}, and the electron identification efficiency ϵ^{eID}. In the TPC-TOF/TPC analyses, ϵ^{geo}, ϵ^{reco}, and ϵ^{eID} in TOF were obtained using a Monte Carlo simulation. Proton-proton events at $\sqrt{s} = 2.76$ TeV were generated with the PYTHIA 6.4.21 event generator [49]. Two samples were used for the efficiency calculation: a minimum bias sample based on the Perugia-0 tune [50] and a heavy-flavor enhanced sample containing only events with at least one $c\bar{c}$ or $b\bar{b}$ pair. The enhanced sample provided a sufficient number of tracks for efficiency determination in the p_T region above 4 GeV/c. Tracks

TABLE I. Summary of the track selection cuts utilized in the different analyses. The same track selection cuts are applied in the TPC-TOF and the TPC analyses.

Analysis p_T range (GeV/c)	TPC-TOF/TPC 0.5–4.5	TPC-EMCal 4.5–12
Number of ITS clusters	≥ 3	≥ 3
SPD layer in which a hit is requested	Both	Any
Number of TPC clusters	≥ 120	≥ 120
Number of TPC clusters in dE/dx calculation	≥ 80	…
Distance of closest approach to the primary vertex in xy	< 1 cm	< 1 cm
Distance of closest approach to the primary vertex in z	< 2 cm	< 2 cm
χ^2/ndf of the momentum fit in the TPC	≤ 4	≤ 4
Ratio of found/findable TPC clusters [43]	≥ 0.6	≥ 0.6

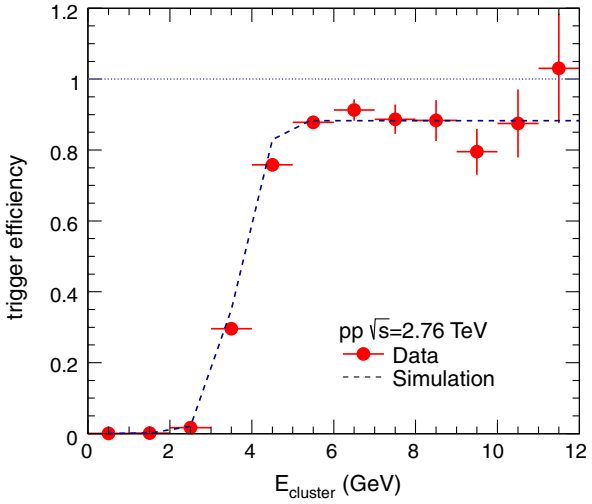

FIG. 1 (color online). Efficiency of the EMCal trigger as a function of the cluster energy measured in the calorimeter [52].

were propagated through the detector using GEANT3 [51]. The electron selection efficiency in the TPC (ϵ_{ID}) was extracted from data using the measured mean $\mathrm{d}E/\mathrm{d}x$ and the width of the $\mathrm{d}E/\mathrm{d}x$ distribution for electrons. The product of acceptance and efficiency was ≈0.3, with a mild dependence on p_{T}. In the TPC-EMCal analysis, the reconstruction efficiency was obtained in a similar way to the TPC-TOF/TPC analyses, and the electron selection efficiency was determined again from data utilizing the measured mean $\mathrm{d}E/\mathrm{d}x$.

In addition, a correction for the trigger bias was applied in the EMCal triggered data sample. This correction was determined from the ratio of the EMCal cluster energy distribution in triggered data compared to those in minimum bias data. The resulting rejection factor at high energy (above the nominal trigger threshold of 3 GeV) was determined to be 1180 ± 10. The trigger efficiency is shown in Fig. 1 as a function of the cluster energy [52]. The trigger efficiency obtained from data is well reproduced by a simulation which incorporated the supermodule-by-supermodule variation in the trigger turn-on curves and took into account the trigger mask employed in data. The statistics of the minimum bias data sample were such that a precise measurement of the trigger efficiency for electrons as a function of track p_{T} was not possible. Thus, the trigger simulation was used to generate a trigger efficiency for electrons as a function of track p_{T}. Above 5 GeV the trigger efficiency is ≈85%, limited by the trigger mask.

The precision of the transverse momentum measurement is limited by the momentum resolution and it is affected by the energy loss of electrons via bremsstrahlung in material. To correct for the resulting distortion of the shape of the inclusive electron p_{T} distributions, an unfolding procedure based on Bayes' theorem [53] was used.

In order to evaluate the systematic uncertainty, the analysis was repeated with modified track selection and particle identification criteria. Table II gives an overview of the systematic uncertainty assigned to various contributions. The total systematic uncertainty of the TPC-TOF/TPC analysis is less than 6% for $p_{\mathrm{T}} < 4.5$ GeV/c. The systematic uncertainty of the TPC-EMCal analysis grows from 10% at 4.5 GeV/c to 20% at 12 GeV/c.

Apart from the signal, the inclusive electron p_{T} spectrum contains background from various sources: conversion of photons including direct photons, Dalitz decays of light mesons, dielectron decays of vector mesons, and semileptonic decays of kaons (K_{e3}). The ratio of signal to background (S/B) depends strongly on p_{T}. While at low p_{T} the background dominates the inclusive electron yield ($S/B \approx 0.2$ at $p_{\mathrm{T}} = 0.5$ GeV/c) the signal becomes more prominent with increasing p_{T} ($S/B > 1$ for $p_{\mathrm{T}} > 2.5$ GeV/c). The background was estimated using a cocktail calculation as described in detail in [19]. The main cocktail input is the measured p_{T}-differential

TABLE II. Contributions to the systematic uncertainties on the inclusive electron spectrum for the different analyses.

Analysis p_{T} range	TPC-TOF/TPC 0.5–4.5 GeV/c	TPC-EMCal 4.5–12 GeV/c
ITS-TPC matching	2%	2%
ITS clusters	3%	3%
TPC clusters	2%	3%
TPC clusters for PID	2%	2%
DCA	Negligible	Negligible
Unfolding	1%	2%
TOF PID	$p_{\mathrm{T}} < 2$ GeV/c: 2%	⋯
TPC PID	$p_{\mathrm{T}} < 4.5$ GeV/c: 2%	⋯
TPC-EMCal PID	⋯	$p_{\mathrm{T}} = 4.5$ GeV/c: 10% $p_{\mathrm{T}} = 12$ GeV/c: 20%
Trigger rejection factor	⋯	3%
Rapidity and charge	2%	2%

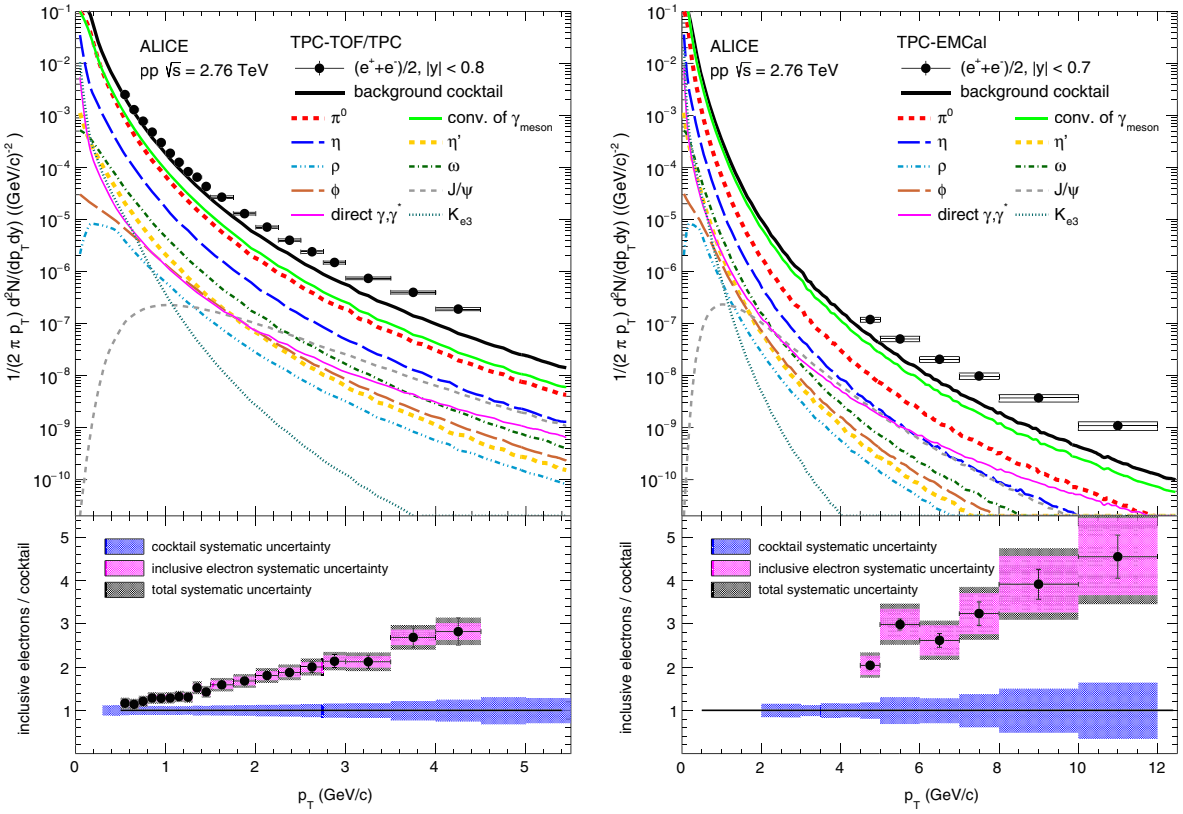

FIG. 2 (color online). p_T-differential invariant yield of inclusive electrons compared to the electron background cocktail for the TPC-TOF/TPC analysis (left) and the TPC-EMCal analysis (right). Ratios of the inclusive electron yields to the respective cocktail are shown in the lower panels.

production cross section of neutral pions [54]. More than 80% of the electron background can be attributed to π^0 Dalitz decays and the conversion of photons from π^0 decays. Other light mesons (η, η', ρ, ω, ϕ) were included via m_T scaling. About 10% of the electron background at high p_T can be attributed to J/ψ decays. The corresponding cocktail input was obtained using a phenomenological interpolation of the J/ψ production cross sections measured at various values of $\sqrt{s}$ as described in [55]. For direct photons an NLO pQCD calculation was used as cocktail input [56,57]. Since the effective material budget was different in the TPC-TOF/TPC and TPC-EMCal analysis due to a different requirement on the hits in the SPD (Table I), the amount of background electrons was different in the two analyses. In order to estimate the systematic uncertainty of the background cocktail, the uncertainties of the various sources were propagated in the cocktail as described in [19]. The total systematic uncertainty of the cocktail in the TPC-TOF/TPC analysis is smallest at $p_T \approx 1.5$ GeV/c where it is ≈7% and increases with increasing p_T reaching 9% at $p_T = 4.5$ GeV/c. At lower p_T the total systematic uncertainty of the cocktail approaches ≈10% at $p_T = 0.5$ GeV/c. The main contribution comes from the uncertainty on the π^0 measurement. In the TPC-EMCal analysis the total systematic uncertainty of the cocktail grows from ≈9% at $p_T = 4.5$ GeV/c to ≈29% at 12 GeV/c. The p_T-differential invariant yield of inclusive electrons is compared to the electron background cocktail in Fig. 2 for the TPC-TOF/TPC analysis (left panel) and the TPC-EMCal analysis (right panel).

The electron background cocktails were statistically subtracted from the inclusive electron p_T distributions obtained in the three analyses. The p_T-differential cross section of electrons from heavy-flavor hadron decays was then obtained by normalizing the invariant yield to the minimum bias cross section, which is 55.4 ± 1.0 mb [58]. The final p_T-differential cross section presented here is a combination of the results from the three analyses as summarized in Table III. In the p_T ranges in which the analyses overlap the results are in agreement within their uncertainties.

TABLE III. Integrated luminosities available for the three analyses based on TPC, TPC-TOF, and TPC-EMCal electron identification, respectively, and kinematical regions covered by these analyses.

Analysis	TPC-TOF	TPC	TPC-EMCal
L_{int} $(nb)^{-1}$	0.8	1.1	12.9
p_T range (GeV/c)	0.5–2	2–4.5	4.5–12
y range	−0.8–0.8	−0.8–0.8	−0.7–0.7

IV. RESULTS

The p_{T}-differential invariant production cross section of electrons from heavy-flavor hadron decays at midrapidity in pp collisions at $\sqrt{s} = 2.76$ TeV is shown in comparison to pQCD calculations from FONLL [36,59,60], GM-VFNS [37–39,61,62], and k_{T}-factorization [40,63–71] in Fig. 3. Statistical and systematic uncertainties of the data are shown separately as error bars and boxes, respectively. Dashed lines indicate the uncertainties of the pQCD calculations originating from the variation of the factorization and normalization scale as well as of the heavy-quark masses [36,38–40]. As seen in the lower panels of Fig. 3, all pQCD calculations are consistent with the measured cross section over the full p_{T} range within combined experimental and theoretical uncertainties. According to the FONLL calculation, this range of the electron transverse momentum includes approximately 50% of the charm and 90% of the total beauty cross section at midrapidity. The latter contribution starts to dominate from approximately 4–5 GeV/c towards higher transverse momenta.

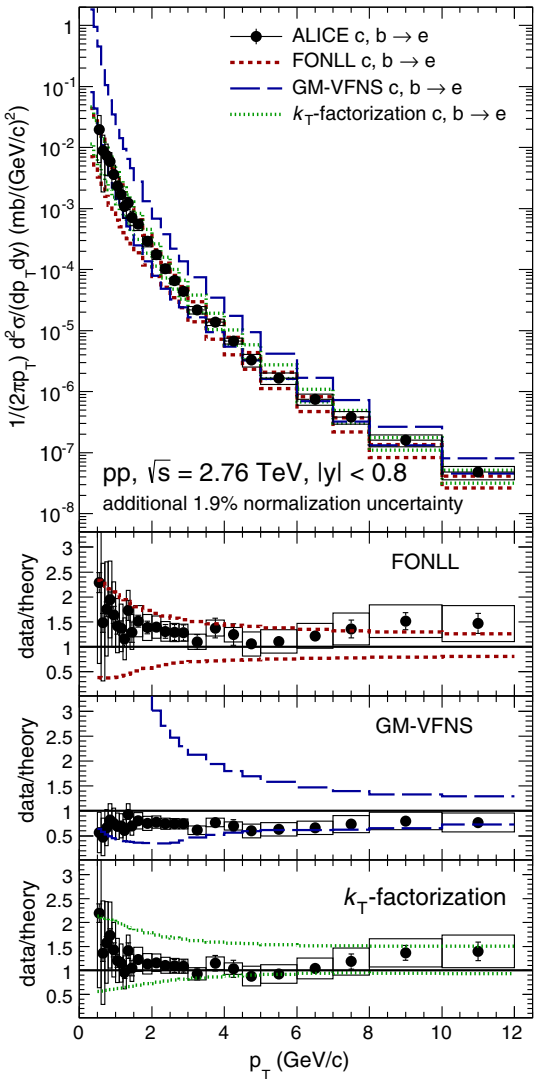

FIG. 3 (color online). p_{T}-differential cross section of electrons from heavy-flavor hadron decays compared to pQCD calculations from FONLL (red) [36,59,60], GM-VFNS (blue) [37–39,61,62] and k_{T}-factorization (green) [40,63–71]. Uncertainties on the theory calculations originate from the variation of the factorization and the renormalization scales and from the heavy-quark masses. The ratios data/theory are shown in the lower panels, where the dashed lines indicate the additional theoretical uncertainties relative to unity.

V. SUMMARY

The inclusive differential production cross section of electrons from charm and beauty hadron decays was measured with ALICE in the transverse momentum range $0.5 < p_{\mathrm{T}} < 12$ GeV/c at midrapidity in pp collisions at $\sqrt{s} = 2.76$ TeV, which is the same center-of-mass energy as the one available so far in Pb-Pb collisions at the LHC. pQCD calculations are in good agreement with the data. The measurement presented in this article improves the reference cross section of electrons from heavy-flavor hadron decays used for the measurement of the corresponding nuclear modification factor in Pb-Pb collisions, where the current reference is obtained by scaling the cross section measured in pp collisions at $\sqrt{s} = 7$ TeV to 2.76 TeV using FONLL pQCD calculations [72].

ACKNOWLEDGMENTS

The ALICE Collaboration would like to thank all its engineers and technicians for their invaluable contributions to the construction of the experiment and the CERN accelerator teams for the outstanding performance of the LHC complex. The ALICE Collaboration gratefully acknowledges the resources and support provided by all Grid centers and the Worldwide LHC Computing Grid (WLCG) collaboration. The ALICE Collaboration would like to thank M. Cacciari, B. A. Kniehl, G. Kramer, R. Maciuła, and A. Szczurek for providing the pQCD predictions for the cross sections of electrons from heavy-flavor hadron decays. Furthermore, the ALICE Collaboration would like to thank W. Vogelsang for providing NLO pQCD predictions for direct photon production cross sections which were used as one of the inputs for the electron background cocktail. The ALICE Collaboration acknowledges the following funding agencies for their support in building and running the ALICE detector: State Committee of Science, World Federation of Scientists (WFS) and Swiss Fonds Kidagan, Armenia, Conselho Nacional de Desenvolvimento Científico e Tecnológico (CNPq), Financiadora de Estudos e Projetos (FINEP), Fundação de Amparo à Pesquisa do Estado de São Paulo (FAPESP); National Natural Science Foundation of China (NSFC), the Chinese Ministry of Education (CMOE) and the Ministry of Science and Technology of China (MSTC); Ministry of Education and Youth of the Czech Republic; Danish Natural

Science Research Council, the Carlsberg Foundation and the Danish National Research Foundation; The European Research Council under the European Community's Seventh Framework Programme; Helsinki Institute of Physics and the Academy of Finland; French CNRS-IN2P3, the "Region Pays de Loire," "Region Alsace," "Region Auvergne" and CEA, France; German Bundesministerium für Bildung und Forschung (BMBF) and the Helmholtz Association; General Secretariat for Research and Technology, Ministry of Development, Greece; Hungarian Orszagos Tudomanyos kutatasi Alapprogramok (OTKA) and National Office for Research and Technology (NKTH); Department of Atomic Energy and Department of Science and Technology of the Government of India; Istituto Nazionale di Fisica Nucleare (INFN) and Centro Fermi–Museo Storico della Fisica e Centro Studi e Ricerche "Enrico Fermi," Italy; MEXT Grant-in-Aid for Specially Promoted Research, Japan; Joint Institute for Nuclear Research, Dubna;); National Research Foundation of Korea (NRF); Consejo Nacional de Ciencia y Tecnologia (CONACYT), Direccion General de Asuntos del Personal Academico (DGAPA), México, Amerique Latine Formation academique - European Commission (ALFA-EC) and the EPLANET Program (European Particle Physics Latin American Network) Stichting voor Fundamenteel Onderzoek der Materie (FOM) and the Nederlandse Organisatie voor Wetenschappelijk Onderzoek (NWO), Netherlands; Research Council of Norway (NFR); Polish Ministry of Science and Higher Education; National Science Centre, Poland; Ministry of National Education/Institute for Atomic Physics and Consiliul National al Cercetarii Stiintifice Unitatea Executiva pentru Finantarea Invatamantului Superior, a Cercetarii Dezvoltarii si Inovarii (CNCS-UEFISCDI)–Romania; Ministry of Education and Science of Russian Federation, Russian Academy of Sciences, Russian Federal Agency of Atomic Energy, Russian Federal Agency for Science and Innovations and The Russian Foundation for Basic Research; Ministry of Education of Slovakia; Department of Science and Technology, South Africa; Centro de Investigaciones Energeticas, MedioAmbiencales y Tecnologicas (CIEMAT), E-Infrastructure shared between Europe and Latin America (EELA), Ministerio de Economía y Competitividad (MINECO) of Spain, Xunta de Galicia (Consellería de Educación), Centro de Aplicaciones Tecnologicas y Desarrollo Nuclear (CEADEN), Cubaenergía, Cuba, and IAEA (International Atomic Energy Agency); Swedish Research Council (VR) and Knut & Alice Wallenberg Foundation (KAW); Ukraine Ministry of Education and Science; United Kingdom Science and Technology Facilities Council (STFC); The United States Department of Energy, the United States National Science Foundation, the State of Texas, and the State of Ohio.

[1] C. Lourenco and H. Woehri, Phys. Rep. **433**, 127 (2006).
[2] R. Averbeck, Prog. Part. Nucl. Phys. **70**, 159 (2013).
[3] I. Arsene *et al.* (BRAHMS Collaboration), Nucl. Phys. **A757**, 1 (2005).
[4] K. Adcox *et al.* (PHENIX Collaboration), Nucl. Phys. **A757**, 184 (2005).
[5] B. Back *et al.* (PHOBOS Collaboration), Nucl. Phys. **A757**, 28 (2005).
[6] J. Adams *et al.* (STAR Collaboration), Nucl. Phys. **A757**, 102 (2005).
[7] B. Abelev *et al.* (ALICE Collaboration), Phys. Lett. B **720**, 52 (2013).
[8] S. Chatrchyan *et al.* (CMS Collaboration), Eur. Phys. J. C **72**, 1945 (2012).
[9] G. Aad *et al.* (ATLAS Collaboration), Phys. Rev. Lett. **105**, 252303 (2010).
[10] A. Adare *et al.* (PHENIX Collaboration), Phys. Rev. Lett. **98**, 172301 (2007).
[11] B. Abelev *et al.* (STAR Collaboration), Phys. Rev. Lett. **98**, 192301 (2007).
[12] B. Abelev *et al.* (ALICE Collaboration), J. High Energy Phys. 09 (2012) 112.
[13] B. Abelev *et al.* (ALICE Collaboration), Phys. Rev. Lett. **109**, 112301 (2012).
[14] Y. Dokshitzer and D. Kharzeev, Phys. Lett. B **519**, 199 (2001).
[15] S. Wicks, W. Horowitz, M. Djordjevic, and M. Gyulassy, Nucl. Phys. **A783**, 493 (2007).
[16] J. Beringer *et al.* (Particle Data Group), Phys. Rev. D **86**, 010001 (2012).
[17] B. Abelev *et al.* (ALICE Collaboration), J. High Energy Phys. 01 (2012) 128.
[18] B. Abelev *et al.* (ALICE Collaboration), Phys. Lett. B **721**, 13 (2013).
[19] B. Abelev *et al.* (ALICE Collaboration), Phys. Rev. D **86**, 112007 (2012).
[20] B. Abelev *et al.* (ALICE Collaboration), Phys. Lett. B **708**, 265 (2012).
[21] B. Abelev *et al.* (ALICE Collaboration), J. High Energy Phys. 11 (2012) 065.
[22] G. Aad *et al.* (ATLAS Collaboration), Phys. Lett. B **707**, 438 (2012).
[23] G. Aad *et al.* (ATLAS Collaboration), Nucl. Phys. **B864**, 341 (2012).
[24] G. Aad *et al.* (ATLAS Collaboration), Nucl. Phys. **B850**, 387 (2011).
[25] V. Khachatryan *et al.* (CMS Collaboration), Eur. Phys. J. C **71**, 1575 (2011).

[26] S. Chatrchyan *et al.* (CMS Collaboration), Phys. Lett. B **714**,136 (2012).
[27] S. Chatrchyan *et al.* (CMS Collaboration), J. High Energy Phys. 06 (2012) 110.
[28] S. Chatrchyan *et al.* (CMS Collaboration), Phys. Rev. D **84**, 052008 (2011).
[29] S. Chatrchyan *et al.* (CMS Collaboration), Phys. Rev. Lett. **106**, 252001 (2011).
[30] V. Khachatryan *et al.* (CMS Collaboration), J. High Energy Phys. 03 (2011) 090.
[31] V. Khachatryan *et al.* (CMS Collaboration), Phys. Rev. Lett. **106**, 112001 (2011).
[32] R. Aaij *et al.* (LHCb Collaboration), J. High Energy Phys. 04 (2012) 093.
[33] R. Aaij *et al.* (LHCb Collaboration), Phys. Lett. B **694**, 209 (2010).
[34] R. Aaij *et al.* (LHCb Collaboration), Eur. Phys. J. C **71**, 1645 (2011).
[35] R. Aaij *et al.* (LHCb Collaboration), Nucl. Phys. **B871**, 1 (2013).
[36] M. Cacciari, S. Frixione, N. Houdeau, M. L. Mangano, P. Nason, and G. Ridolfi, J. High Energy Phys. 10 (2012) 137.
[37] B. Kniehl, G. Kramer, I. Schienbein, and H. Spiesberger, Eur. Phys. J. C **72**, 2082 (2012).
[38] P. Bolzoni and G. Kramer, Nucl. Phys. **B872**, 253 (2013).
[39] P. Bolzoni and G. Kramer, Nucl. Phys. **B876**, 334 (2013).
[40] R. Maciuła and A. Szczurek, Phys. Rev. D **87**, 094022 (2013).
[41] B. Abelev *et al.* (ALICE Collaboration), J. High Energy Phys. 07 (2012) 191.
[42] K. Aamodt *et al.* (ALICE Collaboration), JINST **3**, S08002 (2008).
[43] A. Kalweit, Ph.D. thesis, Technical University Darmstadt, 2012.
[44] K. Aamodt *et al.* (ALICE Collaboration), Phys. Lett. B **693**, 53 (2010).
[45] B. Abelev *et al.* (ALICE Collaboration), Phys. Lett. B **722**, 262 (2013).
[46] J. Allen *et al.* (ALICE EMCal Collaboration), Nucl. Instrum. Methods Phys. Res., Sect. A **615**, 6 (2010).
[47] K. Aamodt *et al.* (ALICE Collaboration), Eur. Phys. J. C **65**, 111 (2010).
[48] J. Alme, Y. Andres, H. Appelshauser, S. Bablok, N. Bialas *et al.*, Nucl. Instrum. Methods Phys. Res., Sect. A **622**,316 (2010).
[49] T. Sjostrand, S. Mrenna, and P. Skands, J. High Energy Phys. 05 (2006) 026.
[50] P. Z. Skands, arXiv:0905.3418; arXiv:0905.3418.
[51] R. Brun *et al.*, CERN Program Library Long Write-up, W5013, 1994.
[52] B. Abelev *et al.* (ALICE Collaboration), Phys. Lett. B **722**, 262 (2013).
[53] G. D'Agostini, Nucl. Instrum. Methods Phys. Res., Sect. A **362**, 487 (1995).
[54] B. Abelev *et al.* (ALICE Collaboration), Eur. Phys. J. C **74**, 3108 (2014).
[55] F. Bossu, Z. C. del Valle, A. de Falco, M. Gagliardi, S. Grigoryan *et al.*, arXiv:1103.2394.
[56] L. Gordon and W. Vogelsang, Phys. Rev. D **48**, 3136 (1993).
[57] L. Gordon and W. Vogelsang, Phys. Rev. D **50**, 1901(1994).
[58] B. Abelev *et al.* (ALICE Collaboration), Eur. Phys. J. C **73**, 2456 (2013).
[59] M. Cacciari, M. Greco, and P. Nason, J. High Energy Phys. 05 (1998) 007.
[60] M. Cacciari, S. Frixione, and P. Nason, J. High Energy Phys. 03 (2001) 006.
[61] B. Kniehl, G. Kramer, I. Schienbein, and H. Spiesberger, Phys. Rev. D **71**, 014018 (2005).
[62] B. Kniehl, G. Kramer, I. Schienbein, and H. Spiesberger, Eur. Phys. J. C **41**, 199 (2005).
[63] P. Hagler, R. Kirschner, A. Schafer, L. Szymanowski, and O. Teryaev, Phys. Rev. D **62**, 071502 (2000).
[64] S. Baranov and M. Smizanska, Phys. Rev. D **62**, 014012 (2000).
[65] S. Baranov, N. Zotov, and A. Lipatov, Phys. At. Nucl. **67**, 837 (2004).
[66] S. Baranov, A. Lipatov, and N. Zotov, Yad. Fiz. **67**, 856 (2004).
[67] H. Jung, M. Kraemer, A. Lipatov, and N. Zotov, J. High Energy Phys. 01 (2011) 085.
[68] H. Jung, M. Kraemer, A. Lipatov, and N. Zotov, Phys. Rev. D **85**, 034035 (2012).
[69] B. Kniehl, A. Shipilova, and V. Saleev, Phys. Rev. D **79**, 034007 (2009).
[70] B. Kniehl, V. Saleev, and A. Shipilova, Phys. Rev. D **81**, 094010 (2010).
[71] V. Saleev and A. Shipilova, Phys. Rev. D **86**, 034032 (2012).
[72] R. Averbeck, N. Bastid, Z. C. del Valle, P. Crochet, A. Dainese *et al.*, arXiv:1107.3243.

B. Abelev,[1] J. Adam,[2] D. Adamová,[3] M. M. Aggarwal,[4] M. Agnello,[5,6] A. Agostinelli,[7] N. Agrawal,[8] Z. Ahammed,[9] N. Ahmad,[10] I. Ahmed,[11] S. U. Ahn,[12] S. A. Ahn,[12] I. Aimo,[5,6] S. Aiola,[13] M. Ajaz,[11] A. Akindinov,[14] S. N. Alam,[9] D. Aleksandrov,[15] B. Alessandro,[5] D. Alexandre,[16] A. Alici,[17,18] A. Alkin,[19] J. Alme,[20] T. Alt,[21] S. Altinpinar,[22] I. Altsybeev,[23] C. Alves Garcia Prado,[24] C. Andrei,[25] A. Andronic,[26] V. Anguelov,[27] J. Anielski,[28] T. Antičić,[29] F. Antinori,[30] P. Antonioli,[18] L. Aphecetche,[31] H. Appelshäuser,[32] N. Arbor,[33] S. Arcelli,[7] N. Armesto,[34] R. Arnaldi,[5] T. Aronsson,[13] I. C. Arsene,[26] M. Arslandok,[32] A. Augustinus,[35] R. Averbeck,[26] T. C. Awes,[36] M. D. Azmi,[37] M. Bach,[21] A. Badalà,[38] Y. W. Baek,[39,40] S. Bagnasco,[5] R. Bailhache,[32] R. Bala,[41] A. Baldisseri,[42] F. Baltasar Dos Santos Pedrosa,[35] R. C. Baral,[43] R. Barbera,[44] F. Barile,[45] G. G. Barnaföldi,[46] L. S. Barnby,[16] V. Barret,[40] J. Bartke,[47] M. Basile,[7] N. Bastid,[40] S. Basu,[9] B. Bathen,[28] G. Batigne,[31] B. Batyunya,[48] P. C. Batzing,[49] C. Baumann,[32] I. G. Bearden,[50] H. Beck,[32] C. Bedda,[6]

N. K. Behera,[8] I. Belikov,[51] F. Bellini,[7] R. Bellwied,[52] E. Belmont-Moreno,[53] R. Belmont III,[54] V. Belyaev,[55] G. Bencedi,[46] S. Beole,[56] I. Berceanu,[25] A. Bercuci,[25] Y. Berdnikov,[57,58] D. Berenyi,[46] M. E. Berger,[59] R. A. Bertens,[60] D. Berzano,[56] L. Betev,[35] A. Bhasin,[41] I. R. Bhat,[41] A. K. Bhati,[4] B. Bhattacharjee,[61] J. Bhom,[62] L. Bianchi,[56] N. Bianchi,[63] C. Bianchin,[60] J. Bielčík,[2] J. Bielčíková,[3] A. Bilandzic,[50] S. Bjelogrlic,[60] F. Blanco,[64] D. Blau,[15] C. Blume,[32] F. Bock,[65,27] A. Bogdanov,[55] H. Bøggild,[50] M. Bogolyubsky,[66] F. V. Böhmer,[59] L. Boldizsár,[46] M. Bombara,[67] J. Book,[32] H. Borel,[42] A. Borissov,[54,68] F. Bossú,[69] M. Botje,[70] E. Botta,[56] S. Böttger,[71] P. Braun-Munzinger,[26] M. Bregant,[24] T. Breitner,[71] T. A. Broker,[32] T. A. Browning,[72] M. Broz,[2] E. Bruna,[5] G. E. Bruno,[45] D. Budnikov,[73] H. Buesching,[32] S. Bufalino,[5] P. Buncic,[35] O. Busch,[27] Z. Buthelezi,[69] D. Caffarri,[74] X. Cai,[75] H. Caines,[13] L. Calero Diaz,[63] A. Caliva,[60] E. Calvo Villar,[76] P. Camerini,[77] F. Carena,[35] W. Carena,[35] J. Castillo Castellanos,[42] E. A. R. Casula,[78] V. Catanescu,[25] C. Cavicchioli,[35] C. Ceballos Sanchez,[79] J. Cepila,[2] P. Cerello,[5] B. Chang,[80] S. Chapeland,[35] J. L. Charvet,[42] S. Chattopadhyay,[9] S. Chattopadhyay,[81] V. Chelnokov,[19] M. Cherney,[82] C. Cheshkov,[83] B. Cheynis,[83] V. Chibante Barroso,[35] D. D. Chinellato,[52] P. Chochula,[35] M. Chojnacki,[50] S. Choudhury,[9] P. Christakoglou,[70] C. H. Christensen,[50] P. Christiansen,[84] T. Chujo,[62] S. U. Chung,[68] C. Cicalo,[85] L. Cifarelli,[7,17] F. Cindolo,[18] J. Cleymans,[37] F. Colamaria,[45] D. Colella,[45] A. Collu,[78] M. Colocci,[7] G. Conesa Balbastre,[33] Z. Conesa del Valle,[86] M. E. Connors,[13] J. G. Contreras,[87] T. M. Cormier,[54] Y. Corrales Morales,[56] P. Cortese,[88] I. Cortés Maldonado,[89] M. R. Cosentino,[24] F. Costa,[35] P. Crochet,[40] R. Cruz Albino,[87] E. Cuautle,[90] L. Cunqueiro,[63] A. Dainese,[30] R. Dang,[75] A. Danu,[91] D. Das,[81] I. Das,[86] K. Das,[81] S. Das,[92] A. Dash,[93] S. Dash,[8] S. De,[9] H. Delagrange,[31,†] A. Deloff,[94] E. Dénes,[46] G. D'Erasmo,[45] A. De Caro,[95,17] G. de Cataldo,[96] J. de Cuveland,[21] A. De Falco,[78] D. De Gruttola,[95,17] N. De Marco,[5] S. De Pasquale,[95] R. de Rooij,[60] M. A. Diaz Corchero,[64] T. Dietel,[28] P. Dillenseger,[32] R. Divià,[35] D. Di Bari,[45] S. Di Liberto,[97] A. Di Mauro,[35] P. Di Nezza,[63] Ø. Djuvsland,[22] A. Dobrin,[60] T. Dobrowolski,[94] D. Domenicis Gimenez,[24] B. Dönigus,[32] O. Dordic,[49] S. Dørheim,[59] A. K. Dubey,[9] A. Dubla,[60] L. Ducroux,[83] P. Dupieux,[40] A. K. Dutta Majumdar,[81] R. J. Ehlers,[13] D. Elia,[96] H. Engel,[71] B. Erazmus,[35,31] H. A. Erdal,[20] D. Eschweiler,[21] B. Espagnon,[86] M. Esposito,[35] M. Estienne,[31] S. Esumi,[62] D. Evans,[16] S. Evdokimov,[66] D. Fabris,[30] J. Faivre,[33] D. Falchieri,[7] A. Fantoni,[63] M. Fasel,[27] D. Fehlker,[22] L. Feldkamp,[28] D. Felea,[91] A. Feliciello,[5] G. Feofilov,[23] J. Ferencei,[3] A. Fernández Téllez,[89] E. G. Ferreiro,[34] A. Ferretti,[56] A. Festanti,[74] J. Figiel,[47] M. A. S. Figueredo,[98] S. Filchagin,[73] D. Finogeev,[99] F. M. Fionda,[45] E. M. Fiore,[45] E. Floratos,[100] M. Floris,[35] S. Foertsch,[69] P. Foka,[26] S. Fokin,[15] E. Fragiacomo,[101] A. Francescon,[35,74] U. Frankenfeld,[26] U. Fuchs,[35] C. Furget,[33] M. Fusco Girard,[95] J. J. Gaardhøje,[50] M. Gagliardi,[56] A. M. Gago,[76] M. Gallio,[56] D. R. Gangadharan,[102] P. Ganoti,[36] C. Garabatos,[26] E. Garcia-Solis,[103] C. Gargiulo,[35] I. Garishvili,[1] J. Gerhard,[21] M. Germain,[31] A. Gheata,[35] M. Gheata,[35,91] B. Ghidini,[45] P. Ghosh,[9] S. K. Ghosh,[92] P. Gianotti,[63] P. Giubellino,[35] E. Gladysz-Dziadus,[47] P. Glässel,[27] A. Gomez Ramirez,[71] P. González-Zamora,[64] S. Gorbunov,[21] L. Görlich,[47] S. Gotovac,[104] L. K. Graczykowski,[105] A. Grelli,[60] A. Grigoras,[35] C. Grigoras,[35] V. Grigoriev,[55] A. Grigoryan,[106] S. Grigoryan,[48] B. Grinyov,[19] N. Grion,[101] J. F. Grosse-Oetringhaus,[35] J.-Y. Grossiord,[83] R. Grosso,[35] F. Guber,[99] R. Guernane,[33] B. Guerzoni,[7] M. Guilbaud,[83] K. Gulbrandsen,[50] H. Gulkanyan,[106] M. Gumbo,[37] T. Gunji,[107] A. Gupta,[41] R. Gupta,[41] K. H. Khan,[11] R. Haake,[28] Ø. Haaland,[22] C. Hadjidakis,[86] M. Haiduc,[91] H. Hamagaki,[107] G. Hamar,[46] L. D. Hanratty,[16] A. Hansen,[50] J. W. Harris,[13] H. Hartmann,[21] A. Harton,[103] D. Hatzifotiadou,[18] S. Hayashi,[107] S. T. Heckel,[32] M. Heide,[28] H. Helstrup,[20] A. Herghelegiu,[25] G. Herrera Corral,[87] B. A. Hess,[108] K. F. Hetland,[20] B. Hippolyte,[51] J. Hladky,[109] P. Hristov,[35] M. Huang,[22] T. J. Humanic,[102] D. Hutter,[21] D. S. Hwang,[110] R. Ilkaev,[73] I. Ilkiv,[94] M. Inaba,[62] G. M. Innocenti,[56] C. Ionita,[35] M. Ippolitov,[15] M. Irfan,[10] M. Ivanov,[26] V. Ivanov,[58] A. Jachołkowski,[44] P. M. Jacobs,[65] C. Jahnke,[24] H. J. Jang,[12] M. A. Janik,[105] P. H. S. Y. Jayarathna,[52] S. Jena,[52] R. T. Jimenez Bustamante,[90] P. G. Jones,[16] H. Jung,[39] A. Jusko,[16] V. Kadyshevskiy,[48] S. Kalcher,[21] P. Kalinak,[111] A. Kalweit,[35] J. Kamin,[32] J. H. Kang,[112] V. Kaplin,[55] S. Kar,[9] A. Karasu Uysal,[113] O. Karavichev,[99] T. Karavicheva,[99] E. Karpechev,[99] U. Kebschull,[71] R. Keidel,[114] M. M. Khan,[115,10] P. Khan,[81] S. A. Khan,[9] A. Khanzadeev,[58] Y. Kharlov,[66] B. Kileng,[20] B. Kim,[112] D. W. Kim,[12,39] D. J. Kim,[80] J. S. Kim,[39] M. Kim,[39] M. Kim,[112] S. Kim,[110] T. Kim,[112] S. Kirsch,[21] I. Kisel,[21] S. Kiselev,[14] A. Kisiel,[105] G. Kiss,[46] J. L. Klay,[116] J. Klein,[27] C. Klein-Bösing,[28] A. Kluge,[35] M. L. Knichel,[26] A. G. Knospe,[117] C. Kobdaj,[35,118] M. K. Köhler,[26] T. Kollegger,[21] A. Kolojvari,[23] V. Kondratiev,[23] N. Kondratyeva,[55] A. Konevskikh,[99] V. Kovalenko,[23] M. Kowalski,[47] S. Kox,[33] G. Koyithatta Meethaleveedu,[8] J. Kral,[80] I. Králik,[111] F. Kramer,[32] A. Kravčáková,[67] M. Krelina,[2] M. Kretz,[21] M. Krivda,[16,111] F. Krizek,[3] E. Kryshen,[35] M. Krzewicki,[26] V. Kučera,[3] Y. Kucheriaev,[15,†] T. Kugathasan,[35] C. Kuhn,[51] P. G. Kuijer,[70] I. Kulakov,[32] J. Kumar,[8] P. Kurashvili,[94] A. Kurepin,[99] A. B. Kurepin,[99] A. Kuryakin,[73] S. Kushpil,[3] M. J. Kweon,[27] Y. Kwon,[112] P. Ladron de Guevara,[90] C. Lagana Fernandes,[24] I. Lakomov,[86] R. Langoy,[119] C. Lara,[71]

A. Lardeux,[31] A. Lattuca,[56] S. L. La Pointe,[60] P. La Rocca,[44] R. Lea,[77] L. Leardini,[27] G. R. Lee,[16] I. Legrand,[35] J. Lehnert,[32] R. C. Lemmon,[120] V. Lenti,[96] E. Leogrande,[60] M. Leoncino,[56] I. León Monzón,[121] P. Lévai,[46] S. Li,[40,75] J. Lien,[119] R. Lietava,[16] S. Lindal,[49] V. Lindenstruth,[21] C. Lippmann,[26] M. A. Lisa,[102] H. M. Ljunggren,[84] D. F. Lodato,[60] P. I. Loenne,[22] V. R. Loggins,[54] V. Loginov,[55] D. Lohner,[27] C. Loizides,[65] X. Lopez,[40] E. López Torres,[79] X.-G. Lu,[27] P. Luettig,[32] M. Lunardon,[74] G. Luparello,[60] C. Luzzi,[35] R. Ma,[13] A. Maevskaya,[99] M. Mager,[35] D. P. Mahapatra,[43] S. M. Mahmood,[49] A. Maire,[27] R. D. Majka,[13] M. Malaev,[58] I. Maldonado Cervantes,[90] L. Malinina,[122,48] D. Mal'Kevich,[14] P. Malzacher,[26] A. Mamonov,[73] L. Manceau,[5] V. Manko,[15] F. Manso,[40] V. Manzari,[96] M. Marchisone,[40,56] J. Mareš,[109] G. V. Margagliotti,[77] A. Margotti,[18] A. Marín,[26] C. Markert,[117] M. Marquard,[32] I. Martashvili,[123] N. A. Martin,[26] P. Martinengo,[35] M. I. Martínez,[89] G. Martínez García,[31] J. Martin Blanco,[31] Y. Martynov,[19] A. Mas,[31] S. Masciocchi,[26] M. Masera,[56] A. Masoni,[85] L. Massacrier,[31] A. Mastroserio,[45] A. Matyja,[47] C. Mayer,[47] J. Mazer,[123] M. A. Mazzoni,[97] F. Meddi,[124] A. Menchaca-Rocha,[53] J. Mercado Pérez,[27] M. Meres,[125] Y. Miake,[62] K. Mikhaylov,[48,14] L. Milano,[35] J. Milosevic,[126,49] A. Mischke,[60] A. N. Mishra,[127] D. Miśkowiec,[26] J. Mitra,[9] C. M. Mitu,[91] J. Mlynarz,[54] N. Mohammadi,[60] B. Mohanty,[128,9] L. Molnar,[51] L. Montaño Zetina,[87] E. Montes,[64] M. Morando,[74] D. A. Moreira De Godoy,[24] S. Moretto,[74] A. Morreale,[80] A. Morsch,[35] V. Muccifora,[63] E. Mudnic,[104] D. Mühlheim,[28] S. Muhuri,[9] M. Mukherjee,[9] H. Müller,[35] M. G. Munhoz,[24] S. Murray,[37] L. Musa,[35] J. Musinsky,[111] B. K. Nandi,[8] R. Nania,[18] E. Nappi,[96] C. Nattrass,[123] K. Nayak,[128] T. K. Nayak,[9] S. Nazarenko,[73] A. Nedosekin,[14] M. Nicassio,[26] M. Niculescu,[35,91] B. S. Nielsen,[50] S. Nikolaev,[15] S. Nikulin,[15] V. Nikulin,[58] B. S. Nilsen,[82] F. Noferini,[17,18] P. Nomokonov,[48] G. Nooren,[60] A. Nyanin,[15] J. Nystrand,[22] H. Oeschler,[27] S. Oh,[13] S. K. Oh,[129,39] A. Okatan,[113] L. Olah,[46] J. Oleniacz,[105] A. C. Oliveira Da Silva,[24] J. Onderwaater,[26] C. Oppedisano,[5] A. Ortiz Velasquez,[84] A. Oskarsson,[84] J. Otwinowski,[26] K. Oyama,[27] P. Sahoo,[127] Y. Pachmayer,[27] M. Pachr,[2] P. Pagano,[95] G. Paić,[90] F. Painke,[21] C. Pajares,[34] S. K. Pal,[9] A. Palmeri,[38] D. Pant,[8] V. Papikyan,[106] G. S. Pappalardo,[38] P. Pareek,[127] W. J. Park,[26] S. Parmar,[4] A. Passfeld,[28] D. I. Patalakha,[66] V. Paticchio,[96] B. Paul,[81] T. Pawlak,[105] T. Peitzmann,[60] H. Pereira Da Costa,[42] E. Pereira De Oliveira Filho,[24] D. Peresunko,[15] C. E. Pérez Lara,[70] A. Pesci,[18] V. Peskov,[32] Y. Pestov,[130] V. Petráček,[2] M. Petran,[2] M. Petris,[25] M. Petrovici,[25] C. Petta,[44] S. Piano,[101] M. Pikna,[125] P. Pillot,[31] O. Pinazza,[18,35] L. Pinsky,[52] D. B. Piyarathna,[52] M. Płoskoń,[65] M. Planinic,[131,29] J. Pluta,[105] S. Pochybova,[46] P. L. M. Podesta-Lerma,[121] M. G. Poghosyan,[35] E. H. O. Pohjoisaho,[132] B. Polichtchouk,[66] N. Poljak,[29] A. Pop,[25] S. Porteboeuf-Houssais,[40] J. Porter,[65] B. Potukuchi,[41] S. K. Prasad,[54] R. Preghenella,[18,17] F. Prino,[5] C. A. Pruneau,[54] I. Pshenichnov,[99] G. Puddu,[78] P. Pujahari,[54] V. Punin,[73] J. Putschke,[54] H. Qvigstad,[49] A. Rachevski,[101] S. Raha,[92] J. Rak,[80] A. Rakotozafindrabe,[42] L. Ramello,[88] R. Raniwala,[133] S. Raniwala,[133] S. S. Räsänen,[132] B. T. Rascanu,[32] D. Rathee,[4] A. W. Rauf,[11] V. Razazi,[78] K. F. Read,[123] J. S. Real,[33] K. Redlich,[134,94] R. J. Reed,[13] A. Rehman,[22] P. Reichelt,[32] M. Reicher,[60] F. Reidt,[35] R. Renfordt,[32] A. R. Reolon,[63] A. Reshetin,[99] F. Rettig,[21] J.-P. Revol,[35] K. Reygers,[27] V. Riabov,[58] R. A. Ricci,[135] T. Richert,[84] M. Richter,[49] P. Riedler,[35] W. Riegler,[35] F. Riggi,[44] A. Rivetti,[5] E. Rocco,[60] M. Rodríguez Cahuantzi,[89] A. Rodriguez Manso,[70] K. Røed,[49] E. Rogochaya,[48] S. Rohni,[41] D. Rohr,[21] D. Röhrich,[22] R. Romita,[120] F. Ronchetti,[63] P. Rosnet,[40] A. Rossi,[35] F. Roukoutakis,[100] A. Roy,[127] C. Roy,[51] P. Roy,[81] A. J. Rubio Montero,[64] R. Rui,[77] R. Russo,[56] E. Ryabinkin,[15] Y. Ryabov,[58] A. Rybicki,[47] S. Sadovsky,[66] K. Šafařík,[35] B. Sahlmuller,[32] R. Sahoo,[127] P. K. Sahu,[43] J. Saini,[9] S. Sakai,[65] C. A. Salgado,[34] J. Salzwedel,[102] S. Sambyal,[41] V. Samsonov,[58] X. Sanchez Castro,[51] F. J. Sánchez Rodríguez,[121] L. Šándor,[111] A. Sandoval,[53] M. Sano,[62] G. Santagati,[44] D. Sarkar,[9] E. Scapparone,[18] F. Scarlassara,[74] R. P. Scharenberg,[72] C. Schiaua,[25] R. Schicker,[27] C. Schmidt,[26] H. R. Schmidt,[108] S. Schuchmann,[32] J. Schukraft,[35] M. Schulc,[2] T. Schuster,[13] Y. Schutz,[31,35] K. Schwarz,[26] K. Schweda,[26] G. Scioli,[7] E. Scomparin,[5] R. Scott,[123] G. Segato,[74] J. E. Seger,[82] Y. Sekiguchi,[107] I. Selyuzhenkov,[26] J. Seo,[68] E. Serradilla,[64,53] A. Sevcenco,[91] A. Shabetai,[31] G. Shabratova,[48] R. Shahoyan,[35] A. Shangaraev,[66] N. Sharma,[123] S. Sharma,[41] K. Shigaki,[136] K. Shtejer,[56] Y. Sibiriak,[15] S. Siddhanta,[85] T. Siemiarczuk,[94] D. Silvermyr,[36] C. Silvestre,[33] G. Simatovic,[131] R. Singaraju,[9] R. Singh,[41] S. Singha,[9,128] V. Singhal,[9] B. C. Sinha,[9] T. Sinha,[81] B. Sitar,[125] M. Sitta,[88] T. B. Skaali,[49] K. Skjerdal,[22] M. Slupecki,[80] N. Smirnov,[13] R. J. M. Snellings,[60] C. Søgaard,[84] R. Soltz,[1] J. Song,[68] M. Song,[112] F. Soramel,[74] S. Sorensen,[123] M. Spacek,[2] I. Sputowska,[47] M. Spyropoulou-Stassinaki,[100] B. K. Srivastava,[72] J. Stachel,[27] I. Stan,[91] G. Stefanek,[94] M. Steinpreis,[102] E. Stenlund,[84] G. Steyn,[69] J. H. Stiller,[27] D. Stocco,[31] M. Stolpovskiy,[66] P. Strmen,[125] A. A. P. Suaide,[24] T. Sugitate,[136] C. Suire,[86] M. Suleymanov,[11] R. Sultanov,[14] M. Šumbera,[3] T. Susa,[29] T. J. M. Symons,[65] A. Szabo,[125] A. Szanto de Toledo,[24] I. Szarka,[125] A. Szczepankiewicz,[35] M. Szymanski,[105] J. Takahashi,[93] M. A. Tangaro,[45] J. D. Tapia Takaki,[137,86] A. Tarantola Peloni,[32] A. Tarazona Martinez,[35] M. G. Tarzila,[25] A. Tauro,[35] G. Tejeda Muñoz,[89] A. Telesca,[35] C. Terrevoli,[78] J. Thäder,[26] D. Thomas,[60] R. Tieulent,[83] A. R. Timmins,[52]

A. Toia,[30] H. Torii,[107] V. Trubnikov,[19] W. H. Trzaska,[80] T. Tsuji,[107] A. Tumkin,[73] R. Turrisi,[30] T. S. Tveter,[49] J. Ulery,[32] K. Ullaland,[22] A. Uras,[83] G. L. Usai,[78] M. Vajzer,[3] M. Vala,[111,48] L. Valencia Palomo,[40,86] S. Vallero,[27] P. Vande Vyvre,[35] L. Vannucci,[135] J. Van Der Maarel,[60] J. W. Van Hoorne,[35] M. van Leeuwen,[60] A. Vargas,[89] M. Vargyas,[80] R. Varma,[8] M. Vasileiou,[100] A. Vasiliev,[15] V. Vechernin,[23] M. Veldhoen,[60] A. Velure,[22] M. Venaruzzo,[77,135] E. Vercellin,[56] S. Vergara Limón,[89] R. Vernet,[138] M. Verweij,[54] L. Vickovic,[104] G. Viesti,[74] J. Viinikainen,[80] Z. Vilakazi,[69] O. Villalobos Baillie,[16] A. Vinogradov,[15] L. Vinogradov,[23] Y. Vinogradov,[73] T. Virgili,[95] Y. P. Viyogi,[9] A. Vodopyanov,[48] M. A. Völkl,[27] K. Voloshin,[14] S. A. Voloshin,[54] G. Volpe,[35] B. von Haller,[35] I. Vorobyev,[23] D. Vranic,[26,35] J. Vrláková,[67] B. Vulpescu,[40] A. Vyushin,[73] B. Wagner,[22] J. Wagner,[26] V. Wagner,[2] M. Wang,[75,31] Y. Wang,[27] D. Watanabe,[62] M. Weber,[52] J. P. Wessels,[28] U. Westerhoff,[28] J. Wiechula,[108] J. Wikne,[49] M. Wilde,[28] G. Wilk,[94] J. Wilkinson,[27] M. C. S. Williams,[18] B. Windelband,[27] M. Winn,[27] C. Xiang,[75] C. G. Yaldo,[54] Y. Yamaguchi,[107] H. Yang,[60] P. Yang,[75] S. Yang,[22] S. Yano,[136] S. Yasnopolskiy,[15] J. Yi,[68] Z. Yin,[75] I.-K. Yoo,[68] I. Yushmanov,[15] V. Zaccolo,[50] C. Zach,[2] A. Zaman,[11] C. Zampolli,[18] S. Zaporozhets,[48] A. Zarochentsev,[23] P. Závada,[109] N. Zaviyalov,[73] H. Zbroszczyk,[105] I. S. Zgura,[91] M. Zhalov,[58] H. Zhang,[75] X. Zhang,[75,65] Y. Zhang,[75] C. Zhao,[49] N. Zhigareva,[14] D. Zhou,[75] F. Zhou,[75] Y. Zhou,[60] Zhuo Zhou,[22] H. Zhu,[75] J. Zhu,[75] X. Zhu,[75] A. Zichichi,[17,7] A. Zimmermann,[27] M. B. Zimmermann,[28,35] G. Zinovjev,[19] Y. Zoccarato[83] and M. Zyzak[32]

(ALICE Collaboration)

[1]*Lawrence Livermore National Laboratory, Livermore, California, USA*
[2]*Faculty of Nuclear Sciences and Physical Engineering, Czech Technical University in Prague, Prague, Czech Republic*
[3]*Nuclear Physics Institute, Academy of Sciences of the Czech Republic, Řežu Prahy, Czech Republic*
[4]*Physics Department, Panjab University, Chandigarh, India*
[5]*Sezione INFN, Turin, Italy*
[6]*Politecnico di Torino, Turin, Italy*
[7]*Dipartimento di Fisica e Astronomia dell'Università and Sezione INFN, Bologna, Italy*
[8]*Indian Institute of Technology Bombay (IIT), Mumbai, India*
[9]*Variable Energy Cyclotron Centre, Kolkata, India*
[10]*Department of Physics, Aligarh Muslim University, Aligarh, India*
[11]*COMSATS Institute of Information Technology (CIIT), Islamabad, Pakistan*
[12]*Korea Institute of Science and Technology Information, Daejeon, South Korea*
[13]*Yale University, New Haven, Connecticut, USA*
[14]*Institute for Theoretical and Experimental Physics, Moscow, Russia*
[15]*Russian Research Centre Kurchatov Institute, Moscow, Russia*
[16]*School of Physics and Astronomy, University of Birmingham, Birmingham, United Kingdom*
[17]*Centro Fermi - Museo Storico della Fisica e Centro Studi e Ricerche "Enrico Fermi", Rome, Italy*
[18]*Sezione INFN, Bologna, Italy*
[19]*Bogolyubov Institute for Theoretical Physics, Kiev, Ukraine*
[20]*Faculty of Engineering, Bergen University College, Bergen, Norway*
[21]*Frankfurt Institute for Advanced Studies, Johann Wolfgang Goethe-Universität Frankfurt, Frankfurt, Germany*
[22]*Department of Physics and Technology, University of Bergen, Bergen, Norway*
[23]*V. Fock Institute for Physics, St. Petersburg State University, St. Petersburg, Russia*
[24]*Universidade de São Paulo (USP), São Paulo, Brazil*
[25]*National Institute for Physics and Nuclear Engineering, Bucharest, Romania*
[26]*Research Division and ExtreMe Matter Institute EMMI, GSI Helmholtzzentrum für Schwerionenforschung, Darmstadt, Germany*
[27]*Physikalisches Institut, Ruprecht-Karls-Universität Heidelberg, Heidelberg, Germany*
[28]*Institut für Kernphysik, Westfälische Wilhelms-Universität Münster, Münster, Germany*
[29]*Rudjer Bošković Institute, Zagreb, Croatia*
[30]*Sezione INFN, Padova, Italy*
[31]*SUBATECH, Ecole des Mines de Nantes, Université de Nantes, CNRS-IN2P3, Nantes, France*
[32]*Institut für Kernphysik, Johann Wolfgang Goethe-Universität Frankfurt, Frankfurt, Germany*
[33]*Laboratoire de Physique Subatomique et de Cosmologie, Université Grenoble-Alpes, CNRS-IN2P3, Grenoble, France*
[34]*Departamento de Física de Partículas and IGFAE, Universidad de Santiago de Compostela, Santiago de Compostela, Spain*
[35]*European Organization for Nuclear Research (CERN), Geneva, Switzerland*

[36]*Oak Ridge National Laboratory, Oak Ridge, Tennessee, USA*
[37]*Physics Department, University of Cape Town, Cape Town, South Africa*
[38]*Sezione INFN, Catania, Italy*
[39]*Gangneung-Wonju National University, Gangneung, South Korea*
[40]*Laboratoire de Physique Corpusculaire (LPC), Clermont Université, Université Blaise Pascal, CNRS–IN2P3, Clermont-Ferrand, France*
[41]*Physics Department, University of Jammu, Jammu, India*
[42]*Commissariat à l'Energie Atomique, IRFU, Saclay, France*
[43]*Institute of Physics, Bhubaneswar, India*
[44]*Dipartimento di Fisica e Astronomia dell'Università and Sezione INFN, Catania, Italy*
[45]*Dipartimento Interateneo di Fisica 'M. Merlin' and Sezione INFN, Bari, Italy*
[46]*Wigner Research Centre for Physics, Hungarian Academy of Sciences, Budapest, Hungary*
[47]*The Henryk Niewodniczanski Institute of Nuclear Physics, Polish Academy of Sciences, Cracow, Poland*
[48]*Joint Institute for Nuclear Research (JINR), Dubna, Russia*
[49]*Department of Physics, University of Oslo, Oslo, Norway*
[50]*Niels Bohr Institute, University of Copenhagen, Copenhagen, Denmark*
[51]*Institut Pluridisciplinaire Hubert Curien (IPHC), Université de Strasbourg, CNRS-IN2P3, Strasbourg, France*
[52]*University of Houston, Houston, Texas, USA*
[53]*Instituto de Física, Universidad Nacional Autónoma de México, Mexico City, Mexico*
[54]*Wayne State University, Detroit, Michigan, USA*
[55]*Moscow Engineering Physics Institute, Moscow, Russia*
[56]*Dipartimento di Fisica dell'Università and Sezione INFN, Turin, Italy*
[57]*St. Petersburg State Polytechnical University*
[58]*Petersburg Nuclear Physics Institute, Gatchina, Russia*
[59]*Physik Department, Technische Universität München, Munich, Germany*
[60]*Institute for Subatomic Physics of Utrecht University, Utrecht, Netherlands*
[61]*Gauhati University, Department of Physics, Guwahati, India*
[62]*University of Tsukuba, Tsukuba, Japan*
[63]*Laboratori Nazionali di Frascati, INFN, Frascati, Italy*
[64]*Centro de Investigaciones Energéticas Medioambientales y Tecnológicas (CIEMAT), Madrid, Spain*
[65]*Lawrence Berkeley National Laboratory, Berkeley, California, USA*
[66]*SSC IHEP of NRC Kurchatov institute, Protvino, Russia*
[67]*Faculty of Science, P.J. šafárik University, Košice, Slovakia*
[68]*Pusan National University, Pusan, South Korea*
[69]*iThemba LABS, National Research Foundation, Somerset West, South Africa*
[70]*Nikhef, National Institute for Subatomic Physics, Amsterdam, Netherlands*
[71]*Institut für Informatik, Johann Wolfgang Goethe-Universität Frankfurt, Frankfurt, Germany*
[72]*Purdue University, West Lafayette, Indiana, USA*
[73]*Russian Federal Nuclear Center (VNIIEF), Sarov, Russia*
[74]*Dipartimento di Fisica e Astronomia dell'Università and Sezione INFN, Padova, Italy*
[75]*Central China Normal University, Wuhan, China*
[76]*Sección Física, Departamento de Ciencias, Pontificia Universidad Católica del Perú, Lima, Peru*
[77]*Dipartimento di Fisica dell'Università and Sezione INFN, Trieste, Italy*
[78]*Dipartimento di Fisica dell'Università and Sezione INFN, Cagliari, Italy*
[79]*Centro de Aplicaciones Tecnológicas y Desarrollo Nuclear (CEADEN), Havana, Cuba*
[80]*University of Jyväskylä, Jyväskylä, Finland*
[81]*Saha Institute of Nuclear Physics, Kolkata, India*
[82]*Physics Department, Creighton University, Omaha, Nebraska, USA*
[83]*Université de Lyon, Université Lyon 1, CNRS/IN2P3, IPN-Lyon, Villeurbanne, France*
[84]*Division of Experimental High Energy Physics, University of Lund, Lund, Sweden*
[85]*Sezione INFN, Cagliari, Italy*
[86]*Institut de Physique Nucléaire d'Orsay (IPNO), Université Paris-Sud, CNRS-IN2P3, Orsay, France*
[87]*Centro de Investigación y de Estudios Avanzados (CINVESTAV), Mexico City and Mérida, Mexico*
[88]*Dipartimento di Scienze e Innovazione Tecnologica dell'Università del Piemonte Orientale and Gruppo Collegato INFN, Alessandria, Italy*
[89]*Benemérita Universidad Autónoma de Puebla, Puebla, Mexico*
[90]*Instituto de Ciencias Nucleares, Universidad Nacional Autónoma de México, Mexico City, Mexico*
[91]*Institute of Space Science (ISS), Bucharest, Romania*

[92]Bose Institute, Department of Physics and Centre for Astroparticle Physics and Space Science (CAPSS), Kolkata, India
[93]Universidade Estadual de Campinas (UNICAMP), Campinas, Brazil
[94]National Centre for Nuclear Studies, Warsaw, Poland
[95]Dipartimento di Fisica 'E.R. Caianiello' dell'Università and Gruppo Collegato INFN, Salerno, Italy
[96]Sezione INFN, Bari, Italy
[97]Sezione INFN, Rome, Italy
[98]University of Liverpool, Liverpool, United Kingdom
[99]Institute for Nuclear Research, Academy of Sciences, Moscow, Russia
[100]Physics Department, University of Athens, Athens, Greece
[101]Sezione INFN, Trieste, Italy
[102]Department of Physics, Ohio State University, Columbus, Ohio, USA
[103]Chicago State University, Chicago, Illinois, USA
[104]Technical University of Split FESB, Split, Croatia
[105]Warsaw University of Technology, Warsaw, Poland
[106]A.I. Alikhanyan National Science Laboratory (Yerevan Physics Institute) Foundation, Yerevan, Armenia
[107]University of Tokyo, Tokyo, Japan
[108]Eberhard Karls Universität Tübingen, Tübingen, Germany
[109]Institute of Physics, Academy of Sciences of the Czech Republic, Prague, Czech Republic
[110]Department of Physics, Sejong University, Seoul, South Korea
[111]Institute of Experimental Physics, Slovak Academy of Sciences, Košice, Slovakia
[112]Yonsei University, Seoul, South Korea
[113]KTO Karatay University, Konya, Turkey
[114]Zentrum für Technologietransfer und Telekommunikation (ZTT), Fachhochschule Worms, Worms, Germany
[115]Department of Applied Physics, Aligarh Muslim University, Aligarh, India
[116]California Polytechnic State University, San Luis Obispo, California, USA
[117]The University of Texas at Austin, Physics Department, Austin, Texas, USA
[118]Suranaree University of Technology, Nakhon Ratchasima, Thailand
[119]Vestfold University College, Tonsberg, Norway
[120]Nuclear Physics Group, STFC Daresbury Laboratory, Daresbury, United Kingdom
[121]Universidad Autónoma de Sinaloa, Culiacán, Mexico
[122]M.V. Lomonosov Moscow State University, D.V. Skobeltsyn Institute of Nuclear Physics, Moscow, Russia
[123]University of Tennessee, Knoxville, Tennessee, USA
[124]Dipartimento di Fisica dell'Università 'La Sapienza' and Sezione INFN Rome, Italy
[125]Faculty of Mathematics, Physics and Informatics, Comenius University, Bratislava, Slovakia
[126]University of Belgrade, Faculty of Physics and "Vinča" Institute of Nuclear Sciences, Belgrade, Serbia
[127]Indian Institute of Technology Indore, Indore (IITI), India
[128]National Institute of Science Education and Research, Bhubaneswar, India
[129]Permanent Address: Konkuk University, Seoul, Korea
[130]Budker Institute for Nuclear Physics, Novosibirsk, Russia
[131]University of Zagreb, Zagreb, Croatia
[132]Helsinki Institute of Physics (HIP), Helsinki, Finland
[133]Physics Department, University of Rajasthan, Jaipur, India
[134]Institute of Theoretical Physics, University of Wroclaw, Wroclaw, Poland
[135]Laboratori Nazionali di Legnaro, INFN, Legnaro, Italy
[136]Hiroshima University, Hiroshima, Japan
[137]University of Kansas, Lawrence, Kansas, USA
[138]Centre de Calcul de l'IN2P3, Villeurbanne, France

[†]Deceased.